Anal Bioanal Chem (2010) 397:1997–2011
DOI 10.1007/s00216-010-3669-9

ORIGINAL PAPER

Chiral ligand-exchange separation and resolution of extremely rigid glutamate analogs: 1-aminospiro[2.2]pentyl-1,4-dicarboxylic acids

Benedetto Natalini · Roccaldo Sardella · Nicola Giacchè · Samantha Palmiotto · Emidio Camaioni · Maura Marinozzi · Antonio Macchiarulo · Roberto Pellicciari

Received: 2 February 2010 / Revised: 17 March 2010 / Accepted: 21 March 2010 / Published online: 22 May 2010

Abstract Owing to their chelation ability, a series of fully constrained L-Glu analogs formed by the spiro-union of two cyclopropane rings (1-aminospiro[2.2]pentyl-1,4-dicarboxylic acids, ASPED A–D), was submitted to chiral ligand-exchange chromatographic (CLEC) analysis. As the initial step, two methodologically different chiral devices were evaluated. A chiral stationary phase (CSP) obtained by dynamic coating of C_{18} chains with the *S*-trityl-(*R*)-cysteine ((*R*)-STC) was used first with this objective. The lack of separation of the enantiomers of ASPED C and D prompted us to utilize the chiral mobile phase (CMP) prepared from *O*-benzyl-(*S*)-serine ((*S*)-OBS). The latter afforded complete separation of the four pairs of enantiomers. For all the pairs, quantum mechanical investigations shed light on the main features responsible for the different enantiomer recognition mechanism with (*S*)-OBS. The validated analytical method was then fruitfully adopted for semi-preparative-scale isolation of the enantiomers of ASPED C.

Keywords Glutamate constrained analogs · Coated chiral stationary phase · Chiral mobile phase · Semi-preparative scale-up · Mechanism of chiral recognition

Abbreviations

CLEC	Chiral ligand-exchange chromatography
CSP	Chiral stationary phase
C-CSP	Coated chiral stationary phase
CMP	Chiral mobile phase
ASPED	1-Aminospiro[2.2]pentyl-1,4-dicarboxylic acid
(*S*)-OBS	*O*-Benzyl-(*S*)-serine
(*R*)-STC	*S*-Trityl-(*R*)-cysteine
QM	Quantum mechanical calculations
SCF	Self-consistent field
LOD	Limit of detection
LOQ	Limit of quantification
R^2	Squared regression coefficient
NMDA	*N*-Methyl D-aspartate
rac-Pro	Racemic proline

B. Natalini (✉) · R. Sardella · N. Giacchè · S. Palmiotto · E. Camaioni · M. Marinozzi · A. Macchiarulo · R. Pellicciari
Dipartimento di Chimica e Tecnologia del Farmaco,
Università degli Studi di Perugia,
Via del Liceo 1,
06123 Perugia, Italy
e-mail: natalini@chimfarm.unipg.it

Introduction

In medicinal chemistry, the quest for conformationally constrained analogs of endogenous metabolites is fostered by the notion that these compounds specifically operate on broad populations of biological targets, adopting diverse biologically active conformations in order to selectively interact with the unique binding clefts of protein subtypes [1, 2]. For instance, reduction of the conformational space of L-glutamic acid (L-Glu) by insertion of different ring moieties has been instrumental in the synthesis of chemical tools with improved potency and selectivity at glutamatergic receptors (GluRs) [3–7]. GluRs, in particular, are composed of two families of membrane receptors: ionotropic glutamate receptors (iGluRs) and metabotropic glutamate receptors (mGluRs) [8, 9]. Each family is further divided into multiple and heterogeneous receptor subtypes (AMPA, GluR1-GluR6, KA1-KA2, NMDA, NR1-NR3 in the case of iGluRs, and mGluR1-mGluR8 in the case of mGluRs); all of these contribute to mediation of the pathophysiological

functions of the excitatory amino acid L-Glu in the central nervous system (CNS) [10].

Hence, the availability of potent and selective constrained analogs of L-Glu has significantly contributed to the pharmacological characterization of individual iGluRs and mGluRs in the CNS [11] and to the elucidation of the conformational requirements for selective interaction of L-Glu at each of the GluR subtypes [12–14]. In the framework of a broader project aimed at elucidation of the conformational preferences of L-Glu at glutamate receptors and in a search for new and selective chemical tools, we previously reported the synthesis of 1-aminospiro[2.2]pentyl-1,4-dicarboxylic acids (ASPED A–D, Fig. 1), a series of fully constrained L-Glu analogs formed by the spiro-union of two cyclopropane rings [15]. The four possible racemic diastereoisomers ASPED A–D were prepared by diastereodivergent synthesis. The diastereomers were classified and structurally assigned according to the Gayewski and Burka's rules [16] applying the conventional IUPAC priority and by using crystallographic and NMR studies, respectively. Accordingly, the pair endowed with the shortest distance between the amino group and the distal carboxylic moiety (ASPED A) was named *proximal* whereas that with the largest distance (ASPED D) was named *distal*. The other two isomers were assigned the *medial-syn* (ASPED C) and *medial-anti* (ASPED B) nomenclature depending on orientation above or below the reference plane containing the substituent with the highest priority [15].

Biological appraisal of these compounds showed that only the *medial-anti* and *distal* isomers (ASPED B and ASPED D, respectively) were endowed with moderate affinity for the *N*-methyl D-aspartate (NMDA) receptor whereas no activity at mGluRs was observed for any of the isomers [15].

The chelating feature of these compounds made them suitable for an attempt in their ligand-exchange-based enantiomer discrimination. Interestingly, despite the usual unattractiveness of dealing with chiral mobile phase (CMP) systems, an advantageous specificity emerged when *O*-benzyl-(*S*)-serine ((*S*)-OBS) was used as the chiral selector in the mobile phase. Moreover, fruitful molecular modeling studies enabled rationalization of the different mechanisms of enantiomer discrimination among the four pairs of isomers. Finally, after full validation of the established analytical method, successful ligand-exchange semi-preparative-scale application enabled the separation of the enantiomers of ASPED C.

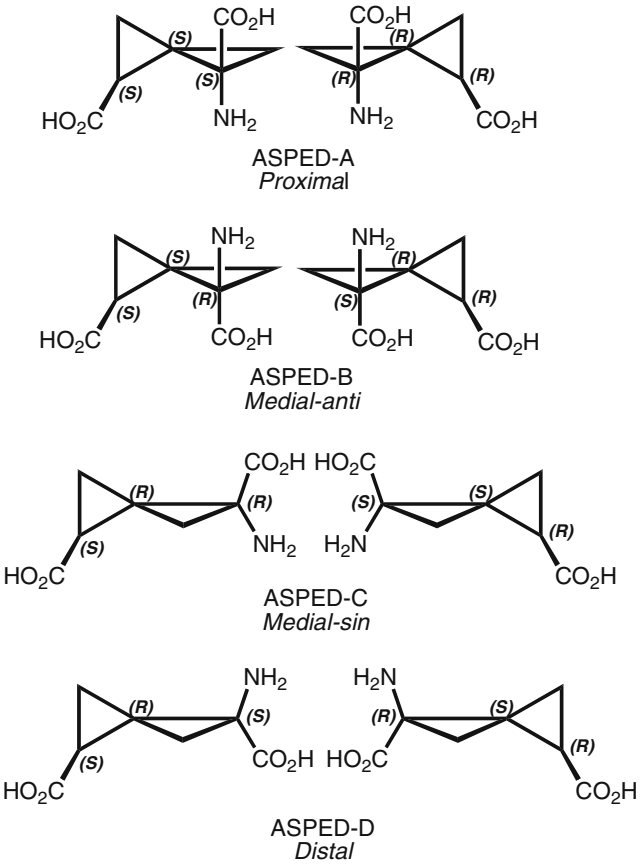

Fig. 1 The structures of the ASPED type analytes investigated

Materials and methods

Chemicals

The Dowex 50W-X2-200 and Dowex 1X8-200 ion-exchange resins and cobalt(II) nitrate hexahydrate, copper (II) nitrate pentahemihydrate, nickel(II) nitrate hexahydrate, zinc(II) nitrate hexahydrate, and the chiral selectors *O*-benzyl-(*S*)-serine ((*S*)-OBS) and *S*-trityl-(*R*)-cysteine ((*R*)-STC) were purchased from Sigma–Aldrich (Milano, Italy). Sodium hydroxide (NaOH), ammonia solution (NH_4OH, 30%), and glacial acetic acid (AcOH) were purchased from Carlo Erba (Rodano, Italy). HPLC-grade water was obtained from a tandem Milli-Ro/Milli-Q apparatus (Millipore, Bedford, MA, USA). All the analytes investigated (namely the four racemic 1-aminospiro[2.2]pentyl-1,4-dicarboxylic acids, ASPEDs, Fig. 1) were synthesized in our laboratories according to the procedure described in Ref. [15]. L-CGA-D, namely (2*S*,1′*S*,2′*R*)-2-(2′-carboxycyclopropyl)glycine, which was utilized as the internal standard, was previously synthesized according to a procedure reported elsewhere [17].

Instrumentation

The analytical HPLC measurements were made on a Shimadzu (Kyoto, Japan) LC-Workstation Class LC-10 equipped with a CBM-10A system controller, two LC-10AD high-pressure binary gradient delivery systems, an SPD-10A variable-wavelength UV–visible detector and a

Rheodyne 7725i injector (Rheodyne, Cotati, CA, USA) with a 20-μL stainless-steel loop. A LiChrospher 100 RP-18 analytical column (Merck, Darmstadt, Germany; 250 mm×4.0 mm i.d., 5 μm, 100 Å) was employed.

For semi-preparative-scale separations, a LiChrospher 100 RP-18 column (Merck, 250 mm×25.0 mm i.d., 5 μm, 100 Å) was utilized.

The semi-preparative HPLC system consisted of a Shimadzu LC-8A pump, a SPD-10Avp variable wavelength UV–visible detector, and a Rheodyne 7725i injector with a 2-mL stainless-steel loop. The chromatographic profile was obtained with Class VP (Shimadzu, ver. 4.3) software.

Dynamic coating with (*R*)-STC and column evaluation

Analytical scale runs were made on a conventional RP-18 analytical column coated with (*R*)-STC. Adsorption of the selector was achieved by recycling a methanol–water solution (250 mL, 75:25 *v*/*v*) of the chiral discriminating agent (0.1 g) for 5 days at 0.5 mL min^{-1}. Before recycling, the chiral selector solution was carefully filtered through a 0.22 mm Millipore filter and degassed with 10 min sonication. With this procedure, an approximate amount of 0.045 g of the selector was established to be hydrophobically bonded to the RP-18 sorbent surface. After washing with a water-methanol solution (50 mL, 98:2, *v*/*v*) in order to displace excess chiral discriminating agent and methanol, the selected copper(II) salt solution was used as the mobile phase. After equilibration for 2 h, the $NaNO_2$ injection peak was used as completely unretained marker in all analyses. Column performance was assessed by periodic injection of racemic proline (*rac*-Pro). The dynamic CSP used in this study was found to be stable and uniformly effective in the chiral separation of amino acids for at least 30 days.

Mobile phase preparation and fixed experimental conditions

Chiral selector: (R)-STC

The mobile phase for the analytical runs was prepared by dissolving Cu(II) nitrate (1.0 mmol L^{-1}) in HPLC-grade water. The resulting solution was filtered through a 0.22-μm Millipore filter and degassed by sonication for 20 min. The sample solutions were prepared at concentrations between approximately 0.1 and 0.5 mg mL^{-1} in filtered mobile phase components and sonicated until completely dissolved. The UV detection wavelengths were set at 254 and 210 nm, and the flow rate was 1.0 mL min^{-1}. The column was then conditioned by recycling the mobile phase for at least 24 h.

Chiral selector: (S)-OBS

The mobile phase for the analytical runs was prepared by dissolving Cu(II) or Co(II) or Zn(II) or Ni(II) nitrate (1.0 mmol L^{-1}) and (*S*)-OBS (2.0 mmol L^{-1}) separately in HPLC-grade water. The resulting solutions were then mixed, filtered through a 0.22-μm Millipore filter and degassed by sonication for 20 min. The sample solutions for the analytical runs were prepared at concentrations between approximately 0.1 and 0.5 mg mL^{-1} in filtered mobile phase components and sonicated until completely dissolved. The analytical column was then conditioned by recycling the selected mobile phase for at least 24 h with a flow rate of 1.0 mL min^{-1}. The UV detection wavelengths were set at 254 and 210 nm.

For the preparative-scale analyses the (*S*)-OBS (2.0 mmol L^{-1}) and only Cu(II) nitrate (1.0 mmol L^{-1}) were used as the mobile-phase components. The mobile phase was prepared in the same way as for the analytical analyses. The optimized ASPED C concentration of 4.5 mg mL^{-1} (with the racemic analyte dissolved in filtered mobile phase) was repeatedly injected for preparative-scale enantiomer separation. The UV detection wavelength was set at 254 nm. Before being injected, the completely solubilized (by sonication) solutions were freshly filtered through 0.22-μm syringe filters (Corning, Germany). A 5.0 mL min^{-1} flow rate was selected with the objective of achieving good chromatographic performance (mainly in terms of resolution factor, R_S) within reasonable analysis time. The semi-preparative column was then conditioned by recycling the selected mobile phase for at least 24 h.

Cation-exchange chromatography

Copper was removed by cation-exchange chromatography. A 300 mm×10 mm i.d. column was packed with Dowex 50W-X2-200 hydrogen, strongly acidic cation-exchange resin and subsequently washed with water until neutral pH. The fractions previously collected during the enantiomer separation process (and characterized by a pale blue color) were concentrated and few drops of concentrated hydrochloric acid were added until pH 1–0 was reached. At this pH, the ternary complex is unstable and the solution loses its color. The chromatography of the copper–analyte–selector mixture thus obtained was performed by washing the resin with water until neutral pH and eluting with 5% ammonia solution. The fractions obtained was checked by TLC and appropriately collected to recover the eluted enantiomer and chiral selector, which were shown to be free from any traces of copper ion.

Anion-exchange chromatography

This step enabled separation of the ASPED C enantiomers from (*S*)-OBS. Dowex 1x8-200 ion-exchange resin was successfully used for this purpose. Before use, the resin (poured into a column like that previously used for the copper-removal procedure) was submitted to treatment aimed at flushing out the constitutive Cl^- anions. This action was carried out by means of 0.3 mol L^{-1} sodium hydroxide solution until the eluate became basic. Chloride anions were then replaced with acetate by flow of 0.3 mol L^{-1} acetic acid solution until the eluate assumed acidic character. Subsequent washing with water adjusted the resin to neutral pH. At this point, the sample dissolved in ammonia solution (pH~9) was first chromatographed with a 0.05 mol L^{-1} acetic acid solution in order to elute the selector from the binary mixture. Subsequently, a more concentrated (0.6 mol L^{-1}) acetic acid solution enabled complete elution of the ASPED C enantiomer. The chromatographic process was followed by TLC. The selected fractions were carefully collected and evaporated to dryness. The same procedure was pursued for the isolation of both ASPED C enantiomers. In this way, pure enantiomers were obtained.

Chromatographic data

All the following chromatographic data were calculated according to the German Pharmacopeia (DAB). The retention factor (k) values were computed by taking the retention time (t_R) at the peak maximum. Enantioseparation factor (α), resolution factor (R_S) and column efficiency (expressed as reduced plate height, h) were computed by use of Eqs. 1–4:

$$\alpha = \frac{k_2}{k_1} \tag{1}$$

$$R_S = 1.18\frac{t_R - t_{Rp}}{W_{0.5} + Wp_{0.5}} \tag{2}$$

$$h = \frac{1000L}{Nd_P} \tag{3}$$

$$N = 5.54\left(\frac{t_R}{W_{0.5}}\right)^2 \tag{4}$$

where k_1 is the retention factor of the first eluted enantiomer, k_2 is the retention factor of the second eluted enantiomer, $W_{0.5}$ is the width of the peak at 50% peak height, $Wp_{0.5}$ is the width of the previous peak at 50% peak height, t_{Rp} is the retention time of the first eluted peak of each pair of enantiomers. N is the number of theoretical plates, L is the length of the column (mm), and d_P is the stationary phase particle diameter.

Computational methods

The structure of the ternary complexes composed of the selector, Cu(II), and the analyte were designed using Maestro 9.0 (Schrödinger ver. 2009, New York, USA) and geometrically optimized in the gas phase using Macromodel 9.7 (Schrödinger ver. 2009) and the OPLS-2005 force. To assess the final energy and geometry more accurately, each resulting complex was further optimized in the gas phase using quantum mechanical (QM) calculations with Jaguar 7.6 (Schrödinger ver. 2009) using the DFT-B3LYP level of theory and the 6-31G** basis-set with the approximation of the self-consistent field (SCF) set at the ultra-fine accuracy level. During all these calculations, a formal charge of +2 and a spin multiplicity of 2 were assigned to each complex.

Results and discussion

In order to select the appropriate chiral selector, the four underivatized racemic ASPEDs were initially analyzed with two methodologically diverse chiral devices. A chiral medium realized by dynamic coating of the C_{18} chains (coated chiral stationary phase, C-CSP) with aralkylic (*R*)-STC [18] molecules, was used first (Fig. 2).

Choice of this chiral selector was based on its proved excellent enantiomer discriminating ability toward physicochemically different classes of amino acids [18–20]. Besides this remarkable effectiveness, the high robustness of this C-CSP was another attractive feature for the purpose of this work. Indeed, in a previous study focused on evaluation of the chromatographic performance of the trityl–cysteine containing mixed stationary phase, the chiral medium performed uniformly for a period of more than 30 days of repeated analyses [18]. In addition to the wide side-chain aromatic portion, the presence of a sulfur atom as the thio-ether spacer between this region and the amino acidic moiety can be additionally invoked to explain the claimed column stability. The four investigated racemic mixtures were thus chromatographed at 1.0 mL min^{-1} mobile phase flow rate and in the presence of a 1.0 mmol L^{-1} Cu(II) nitrate solution. The reason for specific selection of this copper(II) source in the mobile phase is explained below. The chromatographic traces and the values of selected chromatographic data are reported in Table 1.

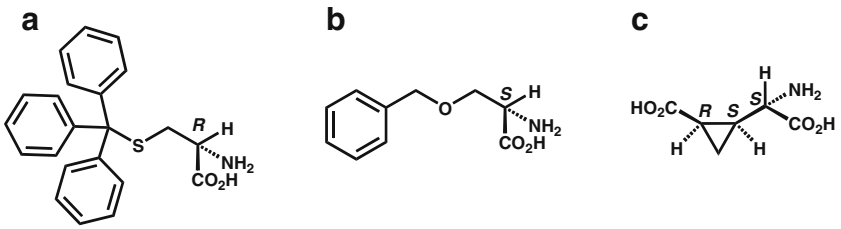

Fig. 2 Structures of (**a**) *S*-trityl-(*R*)-cysteine ((*R*)-STC); (**b**) *O*-benzyl-(*S*)-serine ((*S*)-OBS); (**c**) (2*S*,1′*S*,2′*R*)-2-(2′-carboxycyclopropyl)glycine (L-CGA-D)

Evidently, only the two pairs of enantiomers ASPED A and ASPED B were excellently resolved, the calculated R_S values being 3.36 and 3.49, respectively. In contrast, there was only slight separation of the enantiomers of ASPED C, and no chiral recognition of those of ASPED D. The partial success obtained with the cysteine-based mixed stationary phase prompted us to explore an alternative and conceptually different CLEC approach based on use of a chiral additive to the mobile phase (chiral mobile phase, CMP). (*S*)-OBS [21] was selected as chiral additive, having already been successfully used for discrimination of the enantiomers of acidic amino acids with structural rigidity [21]. In Fig. 3, a schematic experimental flow chart is depicted.

Although physicochemically different, the two chiral selectors are characterized by some structural analogies. First, the free amino acidic moiety in both the species is noteworthy. Moreover, the presence of a heteroatomic spacer between the aromatic area of the selector and its chelating functionality can be also underlined. As far as differences are concerned, more relevant points can be emphasized. In the first instance, the remarkable lipophilicity of (*R*)-STC enables its stable adsorption on to the reversed-phase material, thus giving rise to a reduced number of complexation equilibria as formalized in the scheme below (Eq. 5):

$$\begin{array}{lll} \textit{Mobile phase} & A^m & \\ & \updownarrow & \\ \textit{Stationary phase} & A^s + MC^s & \xleftrightarrow{K^{s}_{AMC}} \quad AMC^s \end{array} \tag{5}$$

where A, M, and C represent the analyte enantiomer, the metal ion, and the chiral selector, respectively, and the superscripts "m" and "s" indicate the residence of the corresponding species in either the mobile or stationary phase, respectively. K_{AMC} represents the formation constant of the analyte–metal ion–chiral selector adduct (AMC) in the two phases.

Conversely, "ubiquitarian" behavior characterizes the serine derivative. Indeed, owing to its aromatic side-chain, (*S*)-OBS also forms hydrophobic layers on the C_{18} chains. However, these interactions are rather unstable [22] and (*S*)-OBS molecules removed from the octadecylsilica based material are continuously replaced by selector molecules in the mobile phase. In accordance to the scheme reported below (Eq. 6) [23], an intricate set of equilibria, which was deeply studied by Kurganov' [24, 25], characterizes such CLEC environments.

$$\begin{array}{lll} \textit{Mobile phase} & A^m + MC^m \xleftrightarrow{K^{m}_{AMC}} & AMC^m \\ & \updownarrow \quad \updownarrow & \updownarrow \\ \textit{Stationary phase} & A^s + MC^s \xleftrightarrow{K^{s}_{AMC}} & AMC^s \end{array} \tag{6}$$

Because of the number of complexation equilibria in Eq. 6, more pronounced variation of overall chromatographic performance on even slight modification of the experimental conditions in these CMP systems, must be expected. The more difficult-to-manage chromatographic event can be reasonably used to explain the scant attractiveness of CMP systems evident from the relatively limited literature. Depending on the experimental conditions adopted, the ligand-exchange processes responsible for enantiomer recognition can mainly occur either on the stationary phase or in the bulk of the solution [26]. However, with 2.0 mmol L^{-1} (*S*)-OBS solution as mobile phase, the complex-formation equilibria can be plausibly hypothesized to be relevant in both chromatographic phases. Moreover, the partitioning of all the species between the two phases must also be taken into account. Despite the emphasized system sophistication and the difficulty of predicting column performance upon even slight modifications of the experimental conditions, a gain in chromatographic performances was achieved by use of 2.0 mmol L^{-1} (*S*)-OBS and 1.0 mmol L^{-1} $Cu(NO_3)_2$ in unbuffered mobile phase, with three out of four enantiomer pairs successfully resolved (Table 2). Indeed, for the three racemates ASPED B, C, and D, appreciable enantiomer resolution was accompanied by excellent R_S values (Table 2). The lack of baseline resolution (R_S=1.03) for the enantiomers of ASPED A prompted us to further explore conditions specifically affecting CLEC recognition.

Table 1 Selected chromatographic data (resolution factor R_S and separation factor α) and chromatographic traces of the investigated racemates obtained with (*R*)-STC as the chiral selector

Samples	R_S	α	Chromatographic traces[a]
ASPED-A (*proximal*)	3.36	1.77	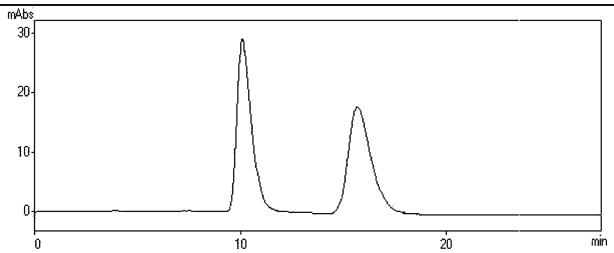
ASPED-B (*medial-anti*)	3.49	1.76	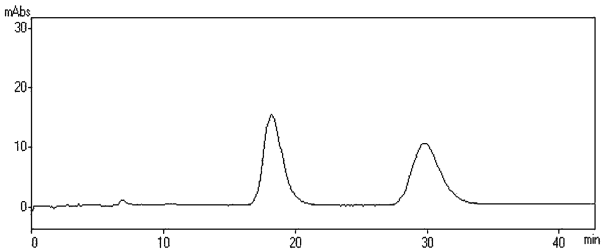
ASPED-C (*medial-syn*)	0.00	1.06	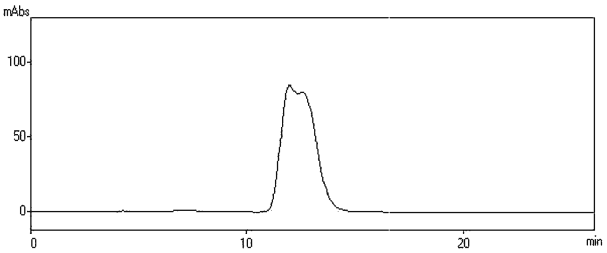
ASPED-D (*distal*)	0.00	1.00	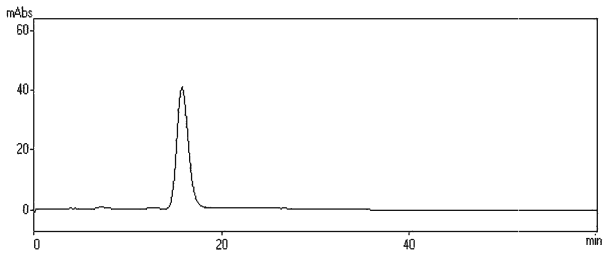

[a] Column: LiChrospher 100 RP-18 (250 mm×4.0 mm i.d., 5 μm, 100 Å); mobile phase: Cu(II) nitrate (1.0 mmol L^{-1}); flow rate: 1.0 mL min^{-1} ; detection: 254 nm

Accordingly, the thermodynamics and kinetics of all the ligand-exchange processes substantially affected by the nature of the central cation and its counter-ion were evaluated. Further, the role of mobile phase flow rate was also investigated. All these experiments are discussed below in separate sections. Moreover, by use of molecular modeling studies, a tentative explanation of the controversial chromatographic behavior of the ASPED A enantiomer pair with the (*S*)-OBS containing system is also reported. Finally, because of the successful analytical separations achieved with the chiral additive to the mobile phase, the method adopted for separation of the enantiomers was fully

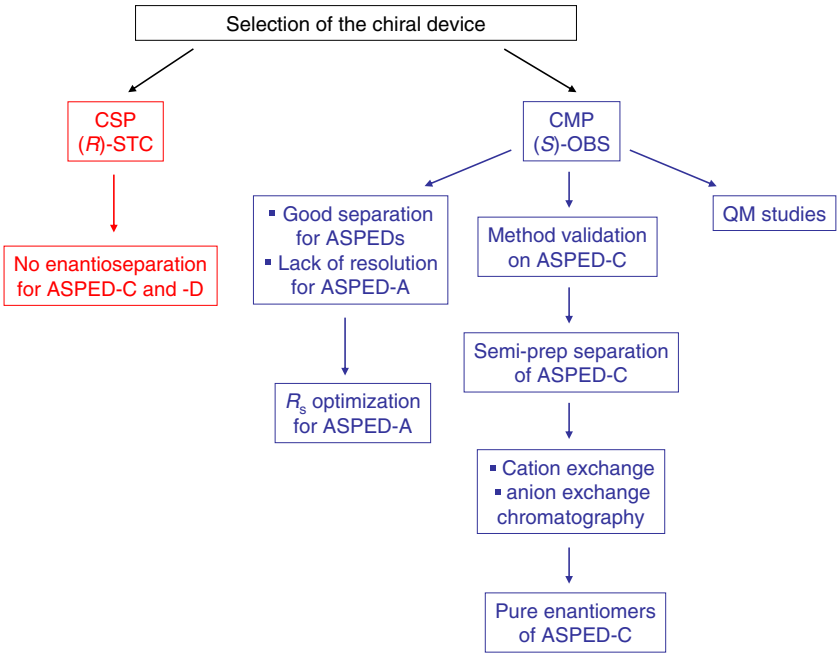

Fig. 3 Block diagram showing the different stages in this work

validated for the ASPED C enantiomer pair only (available in higher amount) which was then separated on a semi-preparative scale.

Selection of the central metal and of its counter-ion for resolution of the enantiomers of ASPED A

Although only scarcely investigated, the nature of the metal counter-ion had a decisive effect on the overall chromatographic performance both when CSP [20] and CMP [21] systems were selected. In this framework, we provided evidence of the noticeable effect of the type of copper salt anion on the separation of the enantiomers of both natural and synthetic amino acids when chromatographed in the presence of (*S*)-OBS as chiral mobile phase additive [21]. Accordingly, when different cupric salts (acetate, nitrate, perchlorate, or sulfate) were coupled with the above chiral additive in an unbuffered system, a noticeable gain of, mainly, R_S was achieved with the Cu (II) nitrate whereas the acetate almost generally furnished the worst results in this respect [21]. With an interest in further exploring the copper salt anion effect, we systematically evaluated a wider set of both organic and inorganic salts by using (*R*)-STC as hydrophobically coated selector for resolution of the enantiomers of amino acidic compounds [20]. Interestingly, despite the above discussed different mechanism of enantiomer recognition between the two chromatographic systems, the copper nitrate was still the elective choice as opposed to copper acetate. A tentative explanation of this intriguing outcome was claimed to be deducible from the following equilibrium (Eq. 7):

$$[selector - Cu(II) - analyte] + Cu(anion)_2 \leftrightarrow \\ \leftrightarrow [selector - Cu(II)]^{+} anion^{-} + [Cu(II) - analyte]^{+} anion^{-} \quad (7)$$

Interference by the copper salt anion with each enantiomer during ternary complex formation was hypothesized [20]. The highest R_S values from the nitrate salt can be assumed to stem from its limited tendency to form complexes in an aqueous system with metal ions [27]. Conversely, the chelating character of the acetate accounts for its pronounced competition with the enantiomer analytes in complexation and hence the low R_S values [28]. Because of the slow kinetics of the ligand-exchange process, any type of interference can affect resolution of the enantiomers, even to a sensitive extent. On the basis of this information, the effect of other anions besides the nitrate upon the resolution of the ASPED A enantiomers was not evaluated. As the next step, replacement of Cu(II) with Co(II), Ni(II) and Zn(II) was evaluated. In strict accordance with literature data, Cu(II) provided the best results because of its ability to form thermodynamically stable and kinetically labile complexes [25, 29], and it must be regarded as the preferred cation for analysis of amino acids [30]. None of the other cations enabled any enantiomer recognition of ASPED A.

Owing to these considerations, Cu(II) nitrate was used during all further analyses aimed at resolving the pair of ASPED A enantiomers.

Table 2 Selected chromatographic data (resolution factor R_S and separation factor α) and chromatographic traces of the investigated racemates obtained with (*S*)-OBS as the chiral selector

Samples	R_S	α	Chromatographic traces[a]
ASPED-A (*proximal*)	1.03	1.10	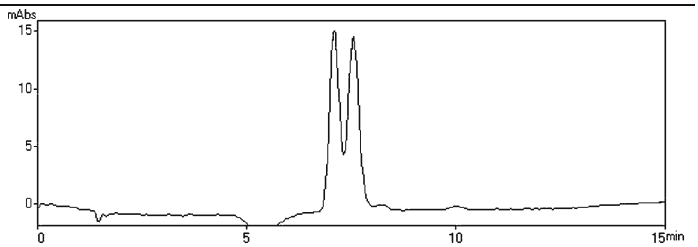
ASPED-B (*medial-anti*)	3.03	1.28	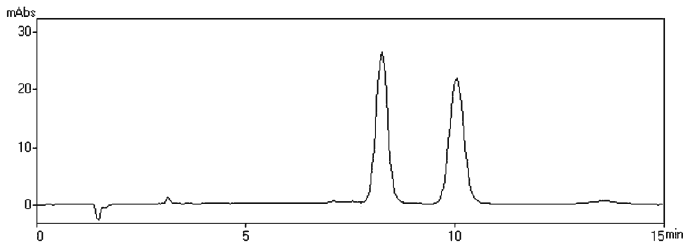
ASPED-C (*medial-syn*)	3.07	1.37	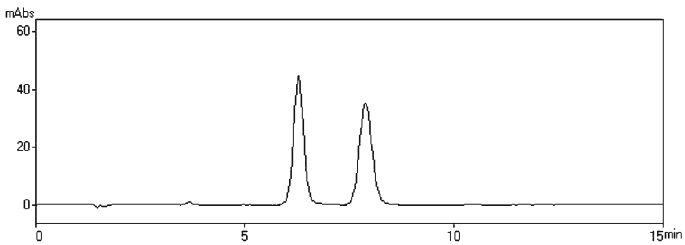
ASPED-D (*distal*)	2.81	1.32	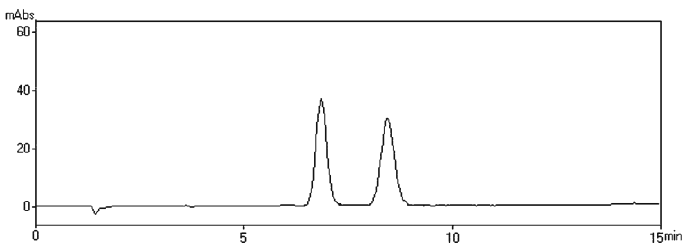

[a] Column: LiChrospher 100 RP-18 (250 mm×4.0 mm i.d., 5 μm, 100 Å); mobile phase: Cu(II) nitrate (1.0 mmol L^{-1}), (*S*)-OBS (2.0 mmol L^{-1}); flow rate: 1.0 mL min^{-1}; detection: 254 nm

Effect of flow rate on resolution of the enantiomers of ASPED A

Modification of the flow rate of the mobile phase often results decisive tuning of overall chromatographic performance. This effect is particularly evident in CLEC systems based on ligand-exchange processes with slow kinetics [31, 32]. In such environments, reduced flow rates enable the exchange processes to be completed, which usually results in higher R_S and lower h values. Accordingly, for both ASPED A peaks, the column efficiency (h) was approximately fivefold better (Table 3) when the mobile phase flow rate was reduced by one order of magnitude (from 1.20 to 0.12 mL min^{-1}). Additionally,

Table 3 Variation of selected chromatographic data (column efficiency h, resolution factor R_S and separation factor α) with mobile phase flow rate for the enantiomer peaks of the ASPED A racemate

Peak #	Flow rate ($mLmin^{-1}$)[a]														
	1.20			1.00			0.50			0.25			0.12		
	h	R_S	α	h	R_S	α	h	R_S	α	h	R_S	α	h	R_S	α
1	89.80			73.63			39.06			25.08			19.65		
		0.82	0.05		1.03	1.10		1.29	1.09		1.64	1.09		1.88	1.09
2	95.40			69.56			38.33			25.03			18.88		

[a] Column: LiChrospher 100 RP-18 (250 mm×4.0 mm i.d., 5 μm, 100 Å); mobile phase: Cu(II) nitrate (1.0 mmol L^{-1}), (*S*)-OBS (2.0 mmol L^{-1}); flow rate: 1.0 mL min^{-1}; detection: 254 nm

an almost doubled value of R_S was obtained (Table 3), which means in this instance baseline separation of the two peaks (Fig. 4). The experimental findings are in agreement with the previous (and generally accepted) assumption that the relatively low efficiency characterizing all CLEC systems is a result of the relative slow exchange kinetics in the column [31, 32]. Moreover, the similarity of the efficiency curves for the two enantiomers, obtained by plotting the reduced plate height (h) against mobile phase velocity (u) (y=65.488x+9.2345 and y=67.974x+7.7042 for the first and second eluted peaks, respectively) indicates analogous phase-exchange kinetics at all the fixed mobile phase flow rates. Worth noting is that variation of the mobile phase velocity did not modify the strength of the stereoselective contacts for the two enantiomers to different extents, which is reflected in the enantioseparation factor (α) being unaffected (Table 3).

Mechanism of chiral recognition

In order to gain insight into the molecular mechanism of chiral recognition of ASPEDs with (*S*)-OBS as chiral selector, quantum mechanical (QM) calculations were performed on the ternary selector–Cu(II)–analyte complexes using the DFT-B3LYP level of theory with the 6-31G** basis set. From a first inspection of the resulting bonding geometries, it is possible to divide the four diastereoisomeric pairs of ASPEDs in two classes according to the number of functional groups involved in coordination of the copper ion by the analyte (Fig. 5). In the first class, the *medial-anti* (ASPED B, Fig. 5c and d) and *distal* (ASPED D, Fig. 5g and h) isomers bind the copper ion using bidentate geometry of coordination that involves the α-amino and α-carboxyl groups of the analyte. In the second class, the *proximal* (ASPED A, Fig. 5a and b) and *medial-syn* (ASPED C, Fig. 5e and f) isomers bind the copper ion using a more energetically favored tridentate geometry of coordination that also involves the participation of the distal carboxylic group of the analyte.

Interestingly, closer examination of members of the second class reveals the presence of two different bonding geometries. While the α-carboxyl group occupies the axial position of coordination on top of the copper ion in the tridentate complexes of ASPED A (Fig. 5a and b), the tridentate complexes of ASPED C (Fig. 5e and f) have more canonical bonding geometry in which the distal carboxyl group is placed in the partly axial position. As a result, the enantiomer pair of ASPED A always form ternary complexes with *cisoid* geometry (Fig. 5a and b) that is at odds with the presence of both *cisoid* and *transoid* geometries in the remaining enantiomeric pairs of ASPEDs. It is likely that the lack of transoid geometry in the enantiomer pair of ASPED A may result

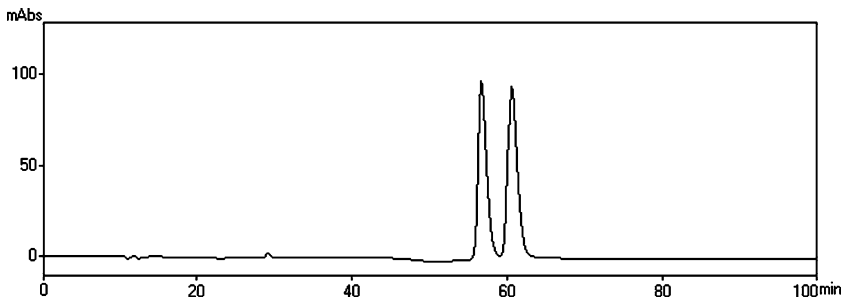

Fig. 4 Chromatographic trace of the ASPED A enantiomers. Column: LiChrospher 100 RP-18 (250 mm×4.0 mm i.d., 5 μm, 100 Å); mobile phase: Cu(II) nitrate (1.0 mmol L^{-1}), (*S*)-OBS (2.0 mmol L^{-1}); flow rate: 0.12 mL min^{-1}; detection: 254 nm

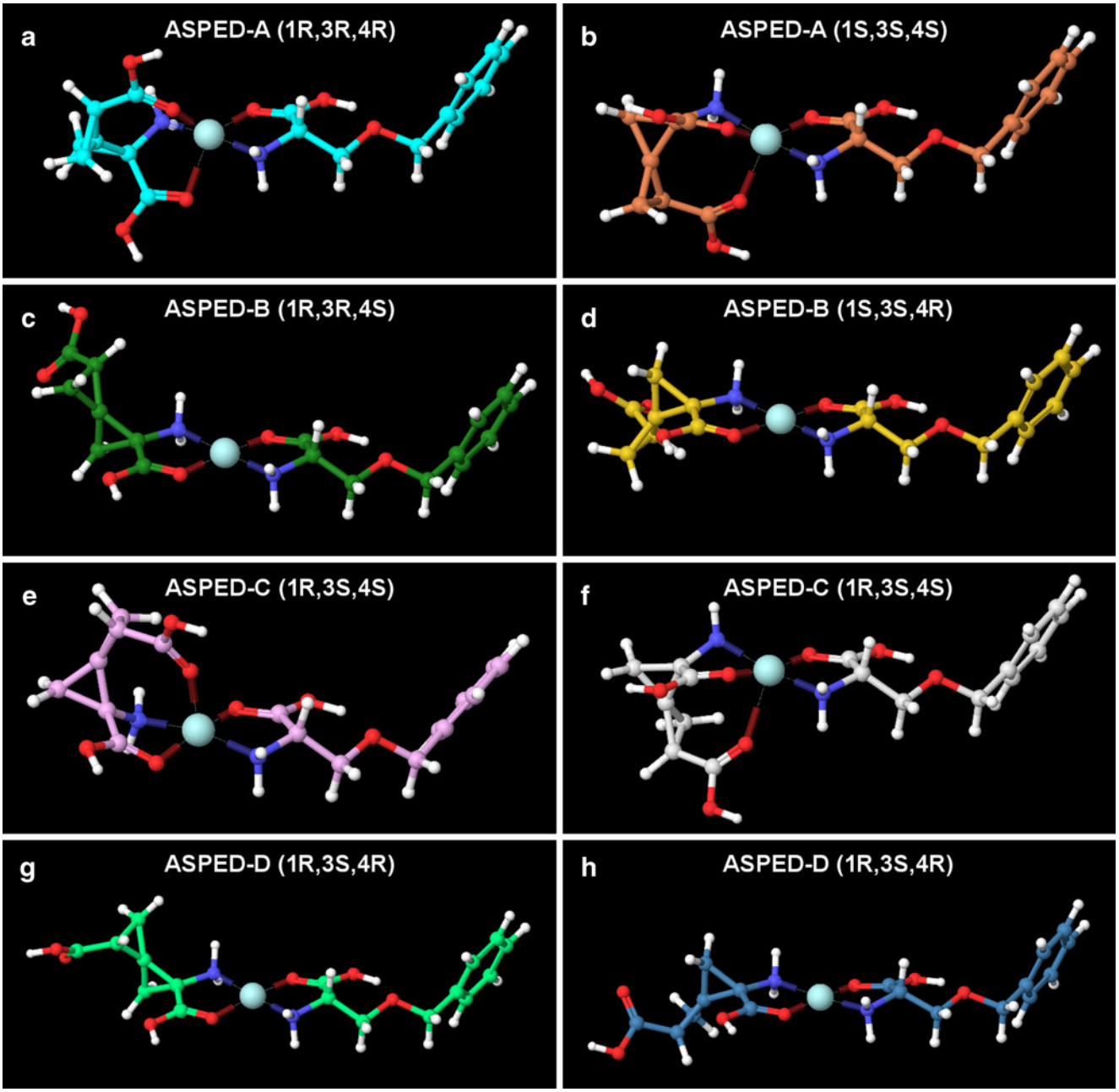

Fig. 5 Three-dimensional structure of the complexes of ASPED A–D with (*S*)-OBS, as resulting from DFT-B3LYP optimization

in cause the absence of selective chiral recognition, thereby hampering the process of separation of these two enantiomers.

Method validation

The chromatographic method in CMP mode was validated over a three-day period. Owing to the limited available amount of the other racemic couples, the following studies were carried out upon the ASPED C enantiomer pair only. However, the outcomes can reasonably be regarded as comparable for all four ASPED racemates investigated.

Selectivity

With the objective of identifying the presence of interferences within the analysis time investigated, three chromatograms of the selected solvent blank (namely the mobile phase) were produced. The peaks obtained (with very small areas in arbitrary units) did not overlap those corresponding to the submitted ASPED C enantiomers.

Moreover, a very appreciable R_S value (2.81) was achieved by using the mobile phase selected. On the basis of these considerations, the results obtained by use of the method can be regarded as selective [33] for ASPED C.

Linearity

With the same modus operandi, independent examinations were conducted on the two ASPED C enantiomers by using six calibration standards. These solutions were prepared as follows: a 100 μg mL^{-1} standard stock solution (consisting of both the ASPED C enantiomers) was diluted to the final individual enantiomer concentrations of 75, 60, 50, 38, 25, and 13 μg mL^{-1}. Moreover, L-CGA-D [17] (Fig. 2) was added as internal standard to all the solutions, always at the final concentration of 85 μg mL^{-1}. To rely upon an internal standard was deemed profitable mainly for correction of injection volume variability. All the calibration standards were analyzed in triplicate. The calibration curves were then constructed by plotting the ratio of the enantiomer-to-internal standard concentrations (as independent variable) against the corresponding peak-area values (in arbitrary units). The mathematical models achieved for the two enantiomers (Eqs. 8 and 9 for the first and second eluted peaks, respectively) were indicative of satisfactory and comparable linearity ($R_{1st}{}^2{}_{peak}$=0.993; $R_{2nd}{}^2{}_{peak}$=0.994) within the concentration range investigated.

$$y = 3.940(\pm 0.085)x - 0.056(\pm 0.048) \quad (8)$$

$$y = 3.559(\pm 0.069)x - 0.013(\pm 0.039) \quad (9)$$

This evidence prompted us to use these regression equations in subsequent estimation of precision, accuracy, and LOD and LOQ.

Intra-day and inter-day precision

Intra-day precision was assessed for both enantiomers of ASPED C by use of the appropriate calibration curves as formalized by Eqs. 8 and 9. An external set of two control solutions (containing both analytes of interest and the internal standard always at a concentration of 85 μg mL^{-1}) were run in triplicate (n=3) within a period of approximately 3 h. The procedure was repeated for a period of three consecutive days. The previously obtained mathematical models were then used to calculate the concentrations of the control solutions. The intra-day precision was then evaluated as the relative standard deviation (*RSD*, %) among the concentration values achieved from each injection.

For each control solution, the variation within replicate injections within a period of three consecutive days (and hence a total of nine injections, n=9) was used to calculate the inter-day precision. In the following discussion, each enantiomer of ASPED C is treated separately. In the first instance, the results obtained for the first eluted peak are examined. Two solutions at concentrations of 42.5 and 32.5 μg mL^{-1} (solutions 1 and 2, respectively) were used as the external set. Lower intra-day precision was encountered for the more concentrated solution (solution 1) with the corresponding *RSD* ranging between 3.3% and 6.0% (Table 4) over the three days.

Lower *RSD* values were obtained for the other enantiomer – within the range 2.7–3.6% (Table 4). However, with the only exception of the *RSD* value estimated for the solution 1 during the third day (6.0%), variation was similar within the investigation period for both external solutions. This is evidence of the stability of the established method for separation of the enantiomers. In accordance with the estimated intra-day precision results, appreciable *RSD* values were also recorded when the long term (inter-day) precision was evaluated. Inherently, although 5.0% variation was computed for solution 1, it was lower for the less concentrated solution 2, the corresponding *RSD* being 3.4% (Table 4).

Identically composed solutions were used for estimation of intra-day and inter-day precision for the second eluted enantiomer. Satisfactory *RSD* values were still obtained for solutions 1 and 2, being 1.8–2.6% and 3.1–6.4% the respective variation intervals (Table 5). Inter-day precision for the second eluted enantiomer was similar to that for the less retained enantiomer, the variation being 4.4% and 5.3% for solutions 1 and 2, respectively (Table 5).

Intra-day and inter-day accuracy

The "Recovery test" approach (percentage recovery) [34] was selected to estimate the accuracy of the adopted CLEC-CMP method. By analogy with the estimation of short and long-term precision discussed above, intra-day and inter-day accuracy was also calculated. Accordingly, while the former was determined by taking into account the three runs for each control solution within a single day (n=3), for the latter, the average value from nine (n=9) determinations (during the three days of analyses) was considered. Following the organization previously adopted for intra-day and inter-day precision, short-term and long-term accuracy are discussed separately. The same external solutions as before were used for the evaluation. For the first eluted ASPED C enantiomer, the intra-day recovery

Table 4 Statistical analysis for the first eluted peak of ASPED C in the short (intra-day) and long (inter-day) period

Solution	Theoretical concentration (±SD; μg mL^{-1})	Intra-day[a]					Inter-day[a]			
		Day	Mean observed concentration (±SD; μg mL^{-1})	n[b]	Precision (*RSD*, %)	Accuracy (Recovery, %)	Mean observed concentration (±SD; μg mL^{-1})	n[b]	Precision (*RSD*, %)	Accuracy (Recovery, %)
1	42.5	1	40.8 (±1.5)	3	3.6	95.9	41.9 (±2.1)	9	5.0	98.6
		2	41.4 (±1.3)		3.3	97.3				
		3	43.6 (±2.6)		6.0	102.7				
2	32.5	1	31.9 (±1.1)	3	3.2	98.0	32.4 (±1.1)	9	3.4	99.6
		2	33.2 (±0.9)		2.7	102.1				
		3	32.0 (±1.2)		3.6	98.6				

[a] Column: LiChrospher 100 RP-18 (250 mm×4.0 mm i.d., 5 μm, 100 Å); mobile phase: Cu(II) nitrate (1.0 mmol L^{-1}), (*S*)-OBS (2.0 mmol L^{-1}); flow rate: 1.0 mL min^{-1}; detection: 254 nm

[b] Number of replicates

ranged between 95.9% and 102.7% for solution 1 (Table 4) whereas variation was between 98.0% and 102.1% for the less concentrated mixture (Table 4).

Long-term (inter-day) recovery was also satisfactory. Indeed, the inter-day accuracy was 98.6% for solution 1 and even better (99.6%) for solution 2 (Table 4). The situation for the more retained enantiomer was no different. For the latter, recovery was 96.9–106.4% for solution 1 and between 100.9% and 108.9% for the, less concentrated, solution 2 (Table 5). Similar accuracy was also obtained in the inter-day study – recovery was 102.6% for solution 1 and 105.5% for solution 2 (Table 5).

Limits of detection (LOD) and quantification (LOQ)

In this study, LOD and LOQ were determined in accordance with the "*Kaiser criterion*" [35]. Low detection and quantification limits were obtained for both enantiomers – 12 ng and 39 ng, respectively, for the first eluted peak, and 11 ng and 35 ng, respectively, for the most retained.

Despite the absence of relevant chromophoric groups in ASPED C (and in all the other mixtures investigated), the appreciably low LOD and LOQ values stem from the marked absorption of all the copper(II)-containing ternary complexes. Moreover, the presence of an aromatic group in the chiral selector (and hence in the eluted diastereomers) must also be considered in explaining these quantities.

The straightforward detectability of aliphatic (and barely UV–visible adsorbing) chelating molecules is, undoubtedly, one of the major attractive features of this CLEC method. Indeed, this is particularly important both when extremely scanty amounts of synthetic (or semi-synthetic) analytes are available or when the type and enantiomer composition of the chelating species from natural matrices need to be investigated at once. In such circumstances, potentially detrimental and time-consuming pre-derivatization processes aimed at inserting suitable UV–visible absorption tags on to the analyte are strongly discouraged. It must be stated, however, that use of spectroscopically non-transparent chiral mobile

Table 5 Statistical analysis for the second eluted peak of ASPED C in the short (intra-day) and long (inter-day) period

Solution	Theoretical concentration (±SD; μg mL^{-1})	Intra-day[a]					Inter-day[a]			
		Day	Mean observed concentration (±SD; μg mL^{-1})	n[b]	Precision (*RSD*, %)	Accuracy (Recovery, %)	Mean observed concentration (±SD; μg mL^{-1})	n[b]	Precision (*RSD*, %)	Accuracy (Recovery, %)
1	42.5	1	41.2 (±0.8)	3	1.8	96.9	43.6 (±1.9)	9	4.4	102.6
		2	44.4 (±1.2)		2.6	104.5				
		3	45.2 (±0.9)		1.9	106.4				
2	32.5	1	32.8 (±1.1)	3	3.4	100.9	34.3 (±1.8)	9	5.3	105.5
		2	35.4 (±1.1)		3.1	108.9				
		3	34.8 (±2.2)		6.4	107.1				

[a] Column: LiChrospher 100 RP-18 (250 mm×4.0 mm i.d., 5 μm, 100 Å); mobile phase: Cu(II) nitrate (1.0 mmol L^{-1}), (*S*)-OBS (2.0 mmol L^{-1}); flow rate: 1.0 mL min^{-1}; detection: 254 nm

[b] Number of replicates

phases (CMPs) could reasonably compromise detection sensitivity [36]. Moreover, the diastereomeric nature of the two eluted ternary complexes could be responsible for the diverse spectroscopic properties and, as a result, different detector responses. This occurrence would unquestionably affect correct analyte quantification (and estimation of enantiomeric excess) [36]. However, while the former drawback can be excluded by selection of an appropriate chiral selector, the latter does not frequently materialize in practice. Consequently, use of CMP systems is a valuable approach to achieving appreciable enantiomer resolution with sensitive detection.

Semi-preparative scale separation of ASPED C enantiomers

During the last decade, semi-preparative CLEC applications in reversed phase (RP) environments have been successfully used for isolation of the enantiomers of chelating compounds with one or more asymmetric carbon centers. Indeed, it is widely accepted that preparative chiral HPLC is often an indispensable aid for resource-intensive, difficult and time-consuming enantioselective synthetic routes. In this scenario, a constant interest was revealed by our group in exploiting CLEC methodology both in C-CSP mode [18] and by using chiral mobile phase additives in the mobile phase [4, 37] for separation of the enantiomers of CNS active compounds.

As the first effort in this direction, relying on the chiral selector *N*,*N*-dimethyl-(*S*)-phenylalanine ((*S*)-DMP) was highly advantageous for obtaining pure enantiomers of the glutamatergic pathway modulator 1-aminoindan-1,5-dicarboxylic acid (AIDA) [37]. The isolated enantiomers (obtained by repeated injection of 5.0–7.0 mg of the racemate and having *ee* of 99.7% for the (*S*) enantiomer and of 98.0% for the (*R*) enantiomer) were used for preliminary physiological and pharmacological evaluation and, for the first time, it was established that only the (*S*) isomer behaves as a potent and mGluRl subtype selective antagonist.

As far as the sample loadability is concerned, a noticeable improvement was achieved by use of a stationary phase operating in the C-CSP mode with (*R*)-STC as chiral selector dynamically coated on to an RP material. Indeed, with this chiral device, up to 15.0 mg *rac*-AIDA can be fully resolved into the pure enantiomers (*ee*≥99.0% for both) with a single injection and with limited run-time [18]. In the course of a following comprehensive study, still with the objective of synthesizing and biologically evaluating new mGluR ligands, the semi-preparative scale CLEC strategy applied in the CMP mode successfully furnished pure enantiomers of another acidic amino acid [4]. Indeed, use of (*S*)-DMP as the chiral additive to the mobile phase also rendered possible the profitable separation of the enantiomers (2*R*) and (2*S*)-(2′,2′-dichloro-3′-carboxybicyclo[1.1.1]pentyl)glycine ((*R*) and (*S*)-DCCBPG). In this case, the two isomers were isolated from a complex matrix which, however, sensitively limited sample loadability. Indeed, despite the excellent enantiomer separation (with α and R_S values of respectively 1.71 and 3.57 on the analytical scale), enantiomer purification from the manifold impurities was possible with replicate injections of no more than 4.0 mg. Nevertheless, pure enantiomeric forms were obtained (both ≥99% *ee*) in sufficient amounts for the preliminary pharmacological assays. Interestingly, these studies revealed, inter alia, that (*S*)-DCCBPG was able to antagonize glutamate-induced responses in both mGlu1 and mGlu5 receptors. Moreover, the (*S*) form was effective at inhibiting NMDA-induced convulsions in vivo when injected intracerebroventricularly in mice.

For CLEC systems the column loadability is lower than that for other enantiodiscriminating materials [38]. Nevertheless, as reported above, even in CLEC systems, repeated in-run injections of enantiomer mixtures can furnish several hundred milligrams of pure enantiomers per day. Further, both the injection and the collection processes can be easily automated. Although good results have been proved, semi-preparative CLEC applications are, however, discouraged for several reasons. First, is the unavoidable step of removing the copper after separation of the enantiomers. However, this can be regarded as a marginal drawback because numerous conceptually different strategies are continuously proposed for this purpose. Indeed, many efforts are specifically devoted to facilitating and rendering more effective the removal of Cu(II) (and, in general, metal ions) from solid wastes, wastewater, etc. For this purpose both “exotic” and easy stratagems have been used [4, 37, 39].

Separation of the chiral selector from the analyte can be seen as another unattractive aspect of the CMP-CLEC semi-preparative scale procedures. The possibility of easily restoring the RP phase, with simple cleaning procedures after use for enantiomer separation allows its successive utilization in the normal way for separation of the selector from the analyte (the isolated enantiomer). The higher the physicochemical difference between selector and selectand (analyte), the easier their RP separation. Moreover, profitable RP purifications are facilitated when selector and selectand have chromophoric groups. The wide commercial availability of cost-effective chiral chelating compounds facilitates appropriate selection in this respect. Conversely, when use of a chiral selector of polarity comparable with that of the analyte and/or a scarce UV adsorption is required, fruitful use of anion-exchange resins is suggested.

Among the main advantages of the CLEC approach, the easy analytical to semi-preparative scale-up is worth mentioning. In accordance with this, several RP analytical

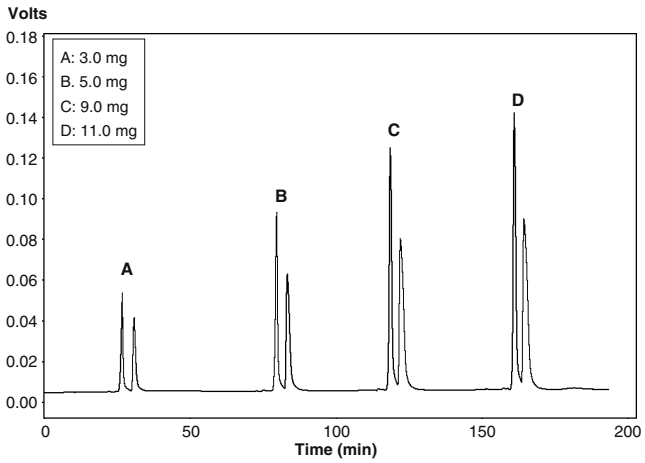

Fig. 6 Chromatographic trace of the ASPED C enantiomers on the semi-preparative scale. CLEC separation with increasing sample concentrations (expressed as mg/2.0 mL). Column: LiChrospher 100 RP-18 (250 mm×25.0 mm i.d., 5 μm, 100 Å); mobile phase: Cu(II) nitrate (1.0 mmol L^{-1}), (*S*)-OBS (2.0 mmol L^{-1}); flow rate: 5.0 mL min^{-1}; detection: 254 nm

and semi-preparative columns with identical constructive and constitutive features are available on the market. This, in turn, enables saving of substantial amounts of time and cost for scale-up procedures. Moreover, separation of the enantiomers of underivatized species in almost all CLEC environments is another major advantage. This is particularly important when only a scanty amount of sample is available for enantiomer resolution. Indeed, risky cleavage steps are profitably avoided. Last but not least, because water is the sole component of many RP CLEC separations (especially when the enantiomers of not particularly hydrophobic compounds must be separated), the whole chromatographic process can be regarded as "eco-friendly". However, the unavoidable need to clean the HPLC apparatus after chromatographic processes with large amounts of water, to preserve parts of the equipment (principally seals and pistons) from an irreversible deterioration, must be pointed out.

Following the same line of research on semi-preparative scale CLEC application, an interest was thus directed toward resolution of the ASPED C racemate, that available in the largest amount. The validated analytical CMP-CLEC method was thus adopted for this purpose. Isolation of the enantiomers of ASPED C enables their separate physicochemical characterization and biological evaluation at the CNS level. Except for the different column dimensions, the conditions used for semi-preparative chromatography were identical with those used for the analytical separation. Indeed, for the occasional separation of this racemate, it was deemed not necessary to further optimize the chromatographic conditions (mainly to improve the α value). Initial experiments were performed to determine the effect of increasing sample load on enantiomer separation. As already mentioned, loading capacity is a critical factor in semi-preparative separations because it determines the maximum amount of sample the column can tolerate without unacceptably compromising the resolution. Accordingly, a series of within-run injections of increasing sample concentrations (specifically, 3.0, 5.0, 9.0 and 11.0 mg dissolved in 2.0 mL mobile phase) was performed (Fig. 6). The racemate was always fully soluble.

As expected, the extent of peak overlap increased as sample loading was increased. The substantially unaffected α value was accompanied by a noticeable drop in R_S on increasing the amount of sample injected (Fig. 7).

Interestingly, the size of the peak of the first eluted enantiomer increased as the sample concentration was increased (Fig. 6) whereas the relative size of the peak of the second eluted isomer remained lower and the peak moved slightly toward the first peak. As reported by Kurganov' [40], different changes in the peak shape especially with increased sample concentrations, can occur when some experimental conditions, for example the Cu(II) content of the mobile phase, are varied. Moreover, the chromatographic behavior was found to be strictly related to the nature of both the analyte and the chiral selector so no generalizations can be made [40]. However, variation of the concentration of the sample injected always results in changes in the concentration of all the of complexes formed in the column. Accordingly, because of the complexity of this CMP-CLEC system (Eq. 6), univocal explanation of the chromatographic outcome is difficult.

On the basis of the loading study, 8.0 mg in the 2.0 mL loop capacity was selected for subsequent runs. This resulted in α and R_S values of 1.02 and 1.90, respectively, and fraction analysis on the CMP-based analytical column revealed very limited overlapping of the enantiomer peaks at the semi-preparative level.

The eluate containing the two peaks, as diastereomeric complexes, was collected and carefully evaporated to dryness. Chromatography on a cation-exchange resin was then

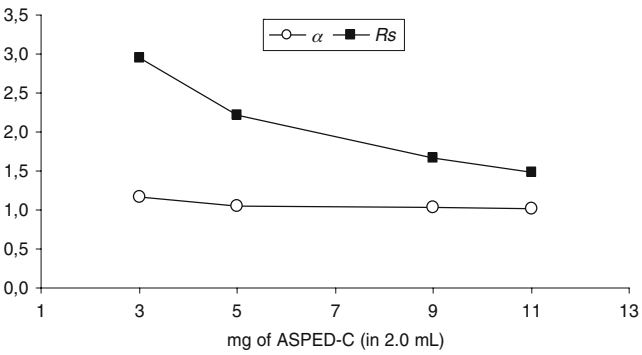

Fig. 7 Variation of the separation (α) and resolution (R_S) factors with increasing ASPED C concentration. Column: LiChrospher 100 RP-18 (250 mm×25.0 mm i.d., 5 μm, 100 Å); mobile phase: Cu(II) nitrate (1.0 mmol L^{-1}), (*S*)-OBS (2.0 mmol L^{-1}); flow rate: 5.0 mL min^{-1}; detection: 254 nm

performed to remove copper(II) from the mixture. The fractions containing the enantiomers and the (*S*)-OBS were then collected and evaporated to give, in both cases, a solid, which was submitted to anion-exchange resin chromatography. As a result of use of the two resins, ca. 17 mg ($[\alpha]_{20}^{D} = +263$, *ee* 99%) and 15 mg ($[\alpha]_{20}^{D} = -247$, *ee* 96%) of the first and second eluted enantiomers, respectively, were obtained.

Concluding remarks

The enantiomers of a series of synthetically available, strongly constrained, L-Glu analogues (ASPED A–D), were successfully separated by CLEC methodology. Initial screening revealed that C-CSP with (*R*)-STC was unable to separate all four pairs of enantiomers. Indeed, excellent enantiomer resolution was obtained for the two species ASPED A and ASPED B only, with only slight separation of the enantiomers of ASPED C and the absence of chiral recognition for those of ASPED D. Overall resolution was, instead, achieved by use of the chiral selector (*S*)-OBS. More specifically, the enantiomers of ASPED B–D were fully resolved (with R_S values of 3.03, 3.07, and 2.81, respectively) under identical experimental conditions; further tuning was necessary to achieve complete enantiomer resolution of ASPED A (R_S= 1.03). The R_S value was increased to 1.88 by reducing the mobile phase flow rate to 0.12 mL min^{-1}. The unusual behavior of this pair was explained by molecular modeling investigations. The diastereomeric complexes of the ASPED A enantiomers were always found to adopt a *cisoid* geometry, in contrast with the presence of both *cisoid* and *transoid* geometries in the ternary assemblies formed by the other ASPED enantiomers. Because the ASPED C enantiomer pair was available in a larger amount than the others, it was used to validate this CLEC method. The low LOD and LOQ values are noteworthy. These very attracting findings enabled successful semi-preparative scale isolation of the enantiomers.

References

1. Pellicciari R, Marinozzi M, Macchiarulo A, Fulco MC, Gafarova J, Serpi M, Giorgi G, Nielsen S, Thomsen C (2007) J Med Chem 50:4630–4641
2. Ahn JM, Gitu PM, Medeiros M, Swift JR, Trivedi D, Hruby VJ (2001) J Med Chem 44:3109–3116
3. Filosa R, Carmela Fulco M, Marinozzi M, Giacchè N, Macchiarulo A, Peduto A, Massa A, de Caprariis P, Thomsen C, Christoffersen CT, Pellicciari R (2009) Bioorg Med Chem 17:242–250
4. Pellicciari R, Filosa R, Fulco MC, Marinozzi M, Macchiarulo A, Novak C, Natalini B, Hermit MB, Nielsen S, Sager TN, Stensbøl TB, Thomsen C (2006) ChemMedChem 1:358–365
5. Pellicciari R, Marinozzi M, Costantino G, Natalini B, Moroni F, Pellegrini-Giampietro D (1999) J Med Chem 42:2716–2720
6. Pellicciari R, Marinozzi M, Natalini B, Costantino G, Luneia R, Giorgi G, Moroni F, Thomsen C (1996) J Med Chem 39:2259–2269
7. Pellicciari R, Luneia R, Costantino G, Marinozzi M, Natalini B, Jakobsen P, Kanstrup A, Lombardi G, Moroni F, Thomsen C (1995) J Med Chem 38:3717–3719
8. Oswald RE, Ahmed A, Fenwick MK, Loh AP (2007) Curr Drug Targets 8:573–582
9. Costantino G, Macchiarulo A, Pellicciari R (2001) Expert Opin Ther Targets 5:669–683
10. Kew JN, Kemp JA (2005) Psychopharmacology 179:4–29
11. Bowie D (2008) CNS Neurol Disord Drug Targets 7:129–143
12. Bessis AS, Jullian N, Coudert E, Pin JP, Acher F (1999) Neuropharmacology 38:1543–1551
13. Costantino G, Macchiarulo A, Pellicciari R (1999) J Med Chem 42:2816–2827
14. Costantino G, Natalini B, Pellicciari R, Moroni F, Lombardi G (1993) Bioorg Med Chem 1:259–265
15. Pellicciari R, Marinozzi M, Camaioni E, del Carmen Nùnez M, Costantino G, Gasparini F, Giorgi G, Macchiarulo A, Subramanian N (2002) J Org Chem 67:5497–5507
16. Gajewski JJ, Burka LT (1970) J Org Chem 35:2190–2196
17. Pellicciari R, Natalini B, Marinozzi M, Selvi L, Chiorri C, Monahan JB, Lanthorn TH, Snyder JP (1988) In: Cavalheiro EA, Lehman J, Turski L (eds) Frontiers in excitatory amino acid research. Alan R. Liss Scientific, Medical and Scholarly Publications, New York
18. Natalini B, Sardella R, Macchiarulo A, Pellicciari R (2008) J Sep Sci 31:696–704
19. Natalini B, Sardella R, Macchiarulo A, Pellicciari R (2008) J Chromatogr B 875:108–117
20. Natalini B, Sardella R, Carbone G, Macchiarulo A, Pellicciari R (2009) Anal Chim Acta 638:225–233
21. Natalini B, Sardella R, Pellicciari R (2005) Curr Anal Chem 1:85–92
22. Natalini B, Sardella R, Macchiarulo A, Pellicciari R (2006) Chirality 18:509–518
23. Davankov VA, Kurganov' AA, Ponomareva TM (1988) J Chromatogr A 452:309–316
24. Kurganov' AA (2001) J Chromatogr A 906:51–71
25. Davankov VA (2003) J Chromatogr A 1000:891–915
26. Galaverna G, Corradini R, Dallavalle F, Folesani G, Dossena A, Marchelli R (2001) J Chromatogr A 922:151–163
27. Diniz V, Volesky B (2005) Water Res 39:2229–2236
28. Wheels AF (1982) Structural inorganic chemistry. Oxford University Press, London
29. Lepri L, Cincinelli A, Del Bubba M (2007) In: Kowalska T, Sherma J (eds) Thin layer chromatography in chiral separations and analysis. Taylor & Francis, Boca Raton
30. Chai Z (2004) In: Cazes J (ed) Encyclopedia of chromatography. Marcel Dekker, New York
31. Davankov VA (1994) J Chromatogr A 666:55–76
32. Remelli M, Trombin D, Conato C (2002) Chromatographia 55:301–306
33. Aboul-Enein HY (2000) Accred Qual Assur 5:180–181
34. González AG, Herrador MA, Asuero AG (1999) Talanta 48:729–736
35. Kaiser H (1965) Fresenius' Z Anal Chem 209:1–18
36. Maier NM, Lindner W (2006) In: Francotte E, Lindner W (eds) Chirality in drug research. Wiley–VCH, Weinheim
37. Natalini B, Marinozzi M, Bade K, Sardella R, Thomsen C, Pellicciari R (2004) Chirality 16:314–317
38. Francotte E (2007) In: Subramanian G (ed) Chiral separation techniques, 3rd edn. Wiley–VCH, Weinheim
39. Nowshuddin S, Reddy AR (2006) Tetrahedron Lett 47:5159–5161
40. Kurganov' AA, Davankov VA, Unger K, Eisenbeiss F, Kinkel J (1994) J Chromatogr A 666:99–110